"How can we improve the coronal field modeling and sciences enhanced with the improved modeling?"

Karel Schrijver (LMSAL)
and the *NLFFF working group**
after five annual meetings

Solar-C Science Definition Meeting ~ Sagamihara ~ 20 Nov. 2008

*Karel Schrijver, Marc DeRosa, *Tom Metcalf*, Graham Barnes, KD Leka, Bruce Lites, Markus Aschwanden, Tahar Amari, Aurélien Canou, Jim McTiernan, Stéphane Régnier, Julia Thalmann, Gherardo Valori, Mike Wheatland, Thomas Wiegelmann, Mark Cheung, Paul Conlon, Marcel Fuhrmann, Bernd Inhester, Tilaye Tadesse*, Aad van Ballegooijen, Kanyo Kusano, Pascal Demoulin, Guillaume Aulanier, Bill Abbett, ...*

Rationale

- Understanding the solar corona requires a *quantitative knowledge of the coronal magnetic field and its currents* to study geometry/topology, energy/currents, connectivity and particle pathways, thermal-energy redistribution, wave guidance, …
- *Nonlinear force-free fields (NLFFFs) are a good approximation* (outside flares/eruptions) in which:

1. The magnetic field is determined inside a computational volume subject to $(\nabla \times \boldsymbol{B}) \times \boldsymbol{B} = 0$, equivalent to $\boldsymbol{J} = \alpha\, \boldsymbol{B}$.
2. The scalar α is invariant along field lines of $\boldsymbol{B}$.
3. In general, α varies spatially: the problem of solving for $\boldsymbol{B}$ is nonlinear.

Algorithms

- Three current classes of NLFFF algorithms:
  - *Optimization*: minimize a metric containing $(\nabla \times \boldsymbol{B}) \times \boldsymbol{B}$ and $\nabla \cdot \boldsymbol{B}$.
  - *Current-field [Grad-Rubin] iteration*: initialize field, apply currents based on surface α, recompute field, iterate…, stop when a fixed point is (hopefully) reached.
  - *Magneto-frictional*: solve an MHD-like system of equations, including an ad-hoc friction in the force term that (hopefully) drives the system toward a force-free state.
- MHD: "relaxed" or evolutionary

Solar study I

- We performed 14 extrapolations for each of two Hinode SOT-SP vector-magnetogram maps bracketing the X flare on 13 Dec. 2006 in AR 10930. *[ApJ 675, 1637 (2008)]*

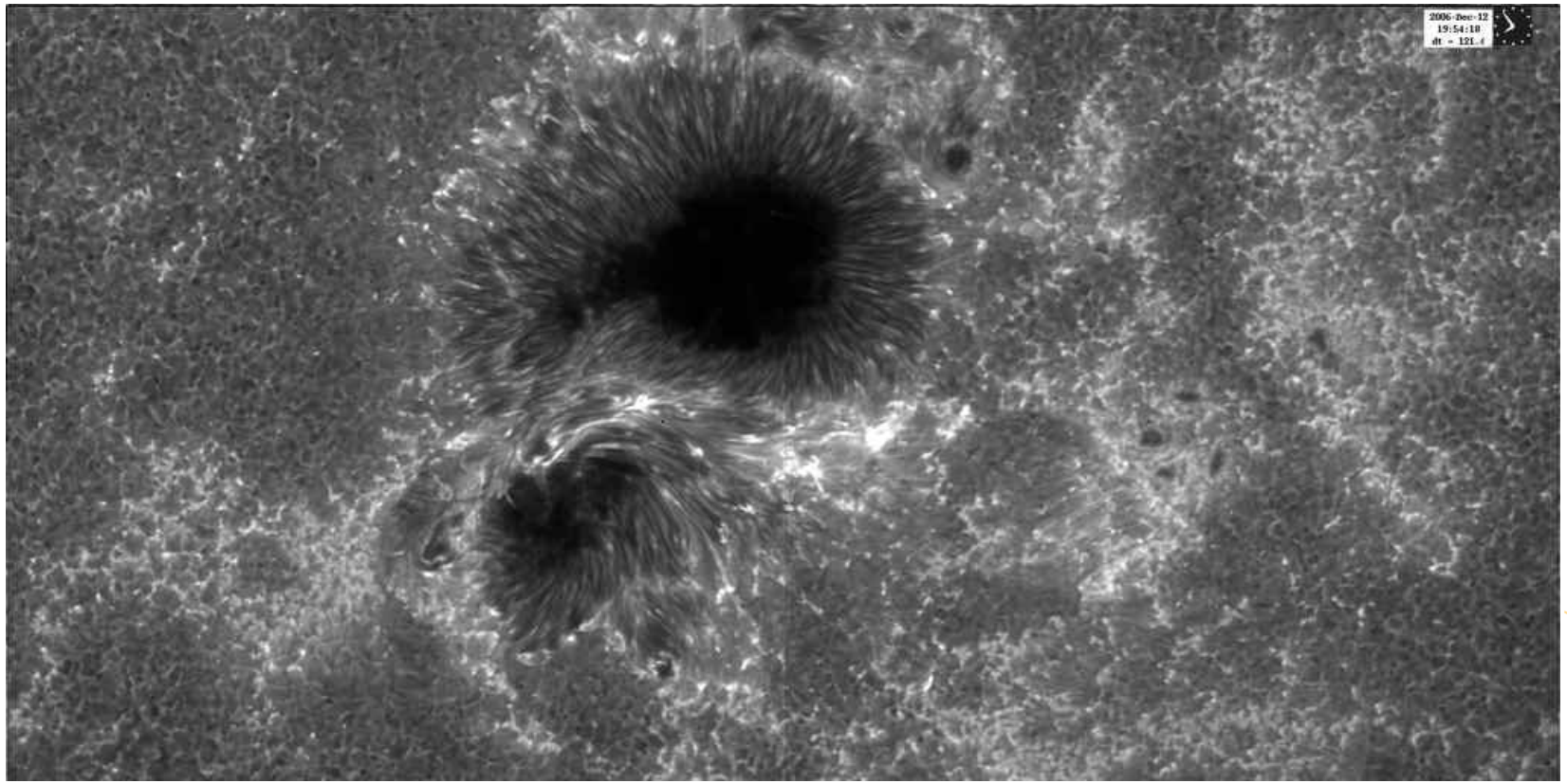

Ca II H from Hinode/SOT-BFI

Hinode/XRT overlay - preflare

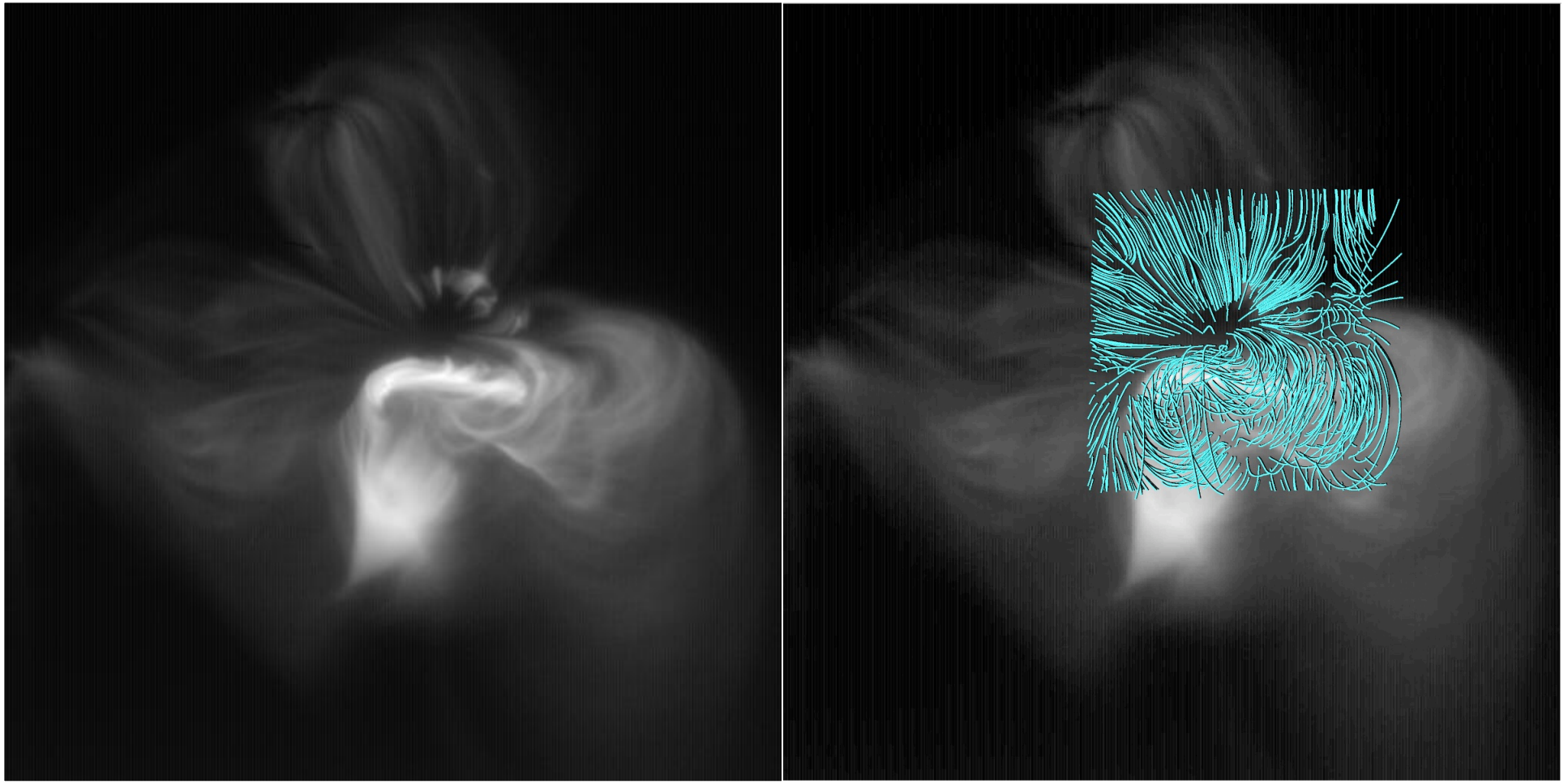

Field lines contained within a 320×320×128-pixel volume

2006.12.12_2030

Volume renderings of current density

pre-flare

post-flare

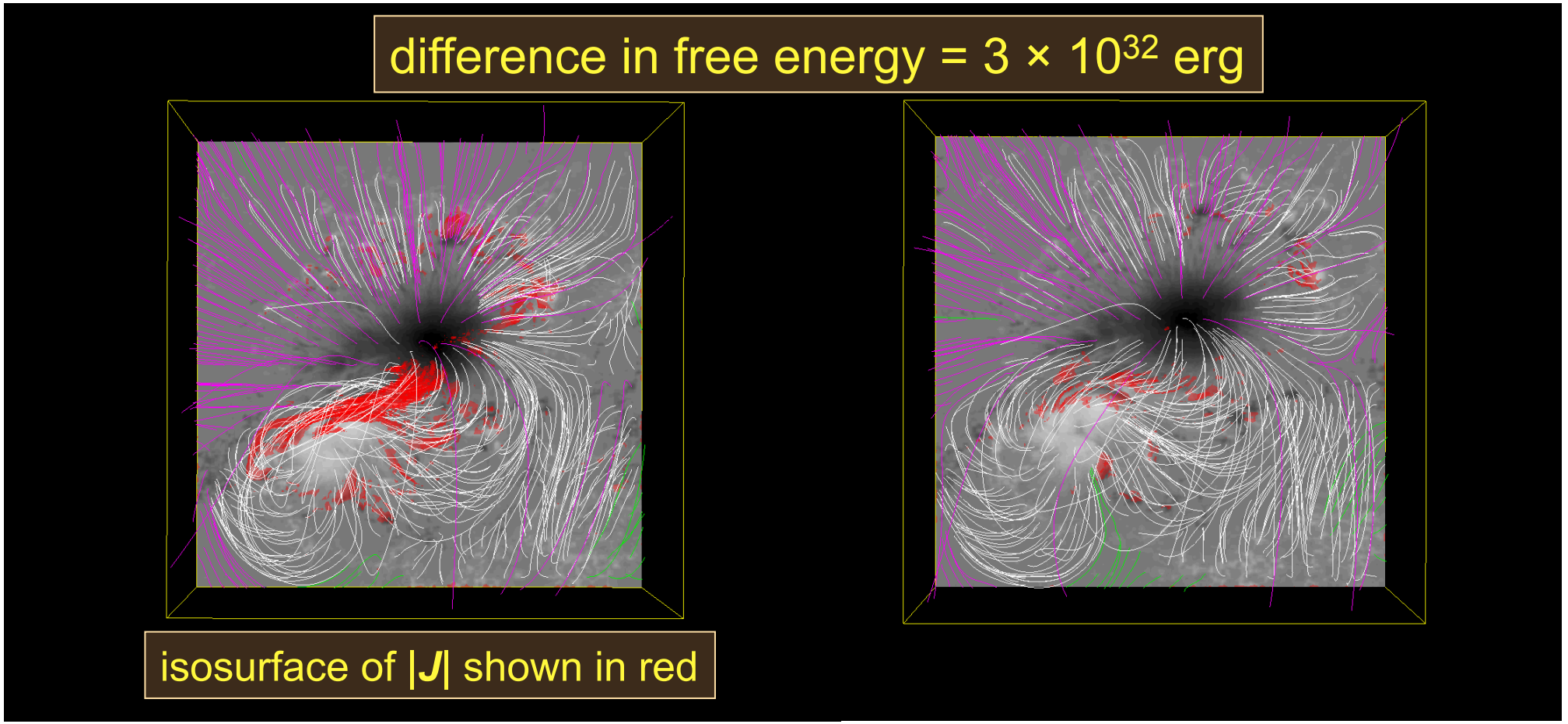

E/E_{pot}=1.32

E/E_{pot}=1.14

Free energies for AR 10930

pre-flare

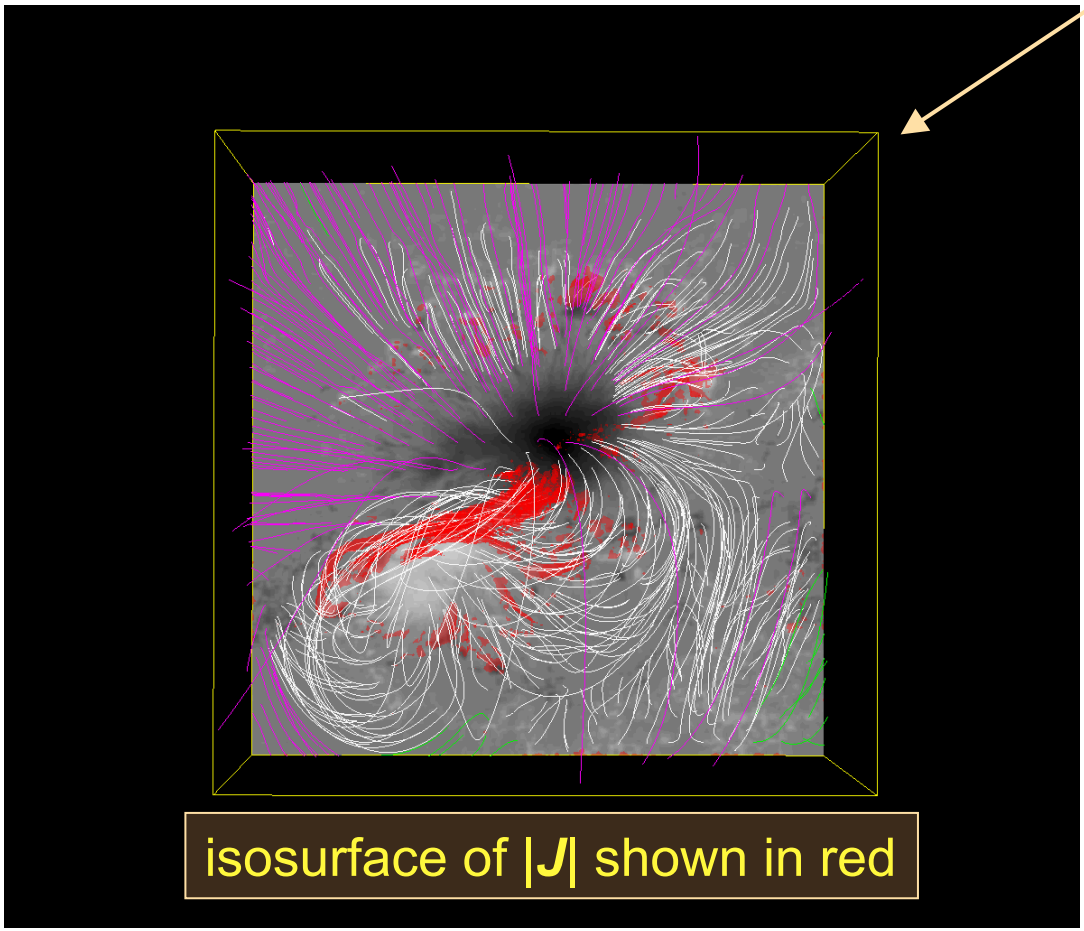

E/E_{pot}=1.32

Model	pre-flare E/E_{pot}
Wh^{+}_{pp}	1.32
Wh^{+}_{np}	1.10
Wie_{wp}	1.09
Val_{pp}	1.10
Wh^{0}_{pp}	1.04
Wie_{ns}	1.04
Val_{np}	0.88
Wie_{np}	0.95
Wie_{pp}	1.05
McT_{pp}	1.01
Wh^{0}_{np}	1.03
Wh^{-}_{np}	1.04
Wh^{-}_{pp}	1.05
McT_{np}	0.95
Potential	1.00

From Table 1 of Schrijver et al. (2008)

Table of metrics for AR 10930

METRICS FOR THE FIELD EXTRAPOLATIONS, IN ORDER OF QUALITY Q BASED ON THE VISUAL CORRESPONDENCE TO THE CORONAL PREFLARE IMAGE

		PREFLARE: 2006 DEC. 12			POSTFLARE: 2006 DEC. 13		
MODEL[1]	Q_m[2]	$E/E_{p,\mathrm{pre}}$[3]	CW $\sin\theta$[4]	$\langle\lvert f_i\rvert\rangle \times 10^{8}$[5]	$E/E_{p,\mathrm{pre}}$	CW $\sin\theta$	$\langle\lvert f_i\rvert\rangle \times 10^{8}$
$\mathrm{Wh}^{+}_{\mathrm{pp}}$	5	1.32	0.24	3.6	1.19	0.18	2.0
$\mathrm{Wh}^{+}_{\mathrm{np}}$	3	1.10	0.27	3.9	1.23	0.27	4.6
$\mathrm{Wie}_{\mathrm{wp}}$	3	1.09	0.35	19	1.18	0.32	13
$\mathrm{Val}_{\mathrm{pp}}$	3	1.10	0.28	230	1.27	0.31	190
$\mathrm{Wh}^{0}_{\mathrm{pp}}$	2	1.04	0.28	3.0	1.53	0.27	3.7
$\mathrm{Wie}_{\mathrm{ns}}$	2	1.04	0.43	22	1.13	0.39	30
$\mathrm{Val}_{\mathrm{np}}$	2	0.88	0.29	220	0.99	0.34	210
$\mathrm{Wie}_{\mathrm{np}}$	1	0.95	0.43	24	1.04	0.39	27
$\mathrm{Wie}_{\mathrm{pp}}$	0	1.05	0.44	18	1.15	0.39	21
$\mathrm{McT}_{\mathrm{pp}}$	0	1.01	0.61	29	1.07	0.59	25
$\mathrm{Wh}^{0}_{\mathrm{np}}$	−1	1.03	0.27	2.5	1.12	0.23	2.6
$\mathrm{Wh}^{-}_{\mathrm{np}}$	−1	1.04	0.25	2.9	1.11	0.24	2.9
$\mathrm{Wh}^{-}_{\mathrm{pp}}$	−1	1.05	0.27	3.2	1.16	0.19	2.2
$\mathrm{McT}_{\mathrm{np}}$	−2	0.95	0.64	26	1.00	0.61	24
Potential	−3	1	...	0.8	1.04	...	0.8

[1] Models: Wh: Wheatland; Wie: Wiegelmann; Val: Valori; McT: McTiernan; +, −, 0: based on positive or negative B_z, or both, respectively; np: no preprocessing; ns: preprocessed without smoothing; pp: preprocessing including smoothing; wp: Wiegelmann's preprocessing and smoothing.

[2] Quality of fit by visual inspection for five features: a good or poor correspondence for each feature adds +1 or −1, respectively, to the total value; an ambiguous correspondence adds 0.

[3] Energy, relative to the energy in the preflare potential field model.

[4] Current-weighted value of $\sin\theta$, where θ is the angle between the electrical current and the magnetic field in the model solution.

[5] The unsigned mean over all pixels i in the comparison volume of the absolute fractional flux change $|f_i| = |(\nabla \cdot \boldsymbol{B})_i|/(6|\boldsymbol{B}|_i/\Delta x)$, where Δx is the grid spacing (cf. Wheatland et al. 2000).

Schrijver et al. (2008)

Summary for AR 10930

- In the best-matching model for the 2006 Dec 13 flare, *free energy drops from 32% to 14% of potential energy, corresponding to a drop in free energy of* 3×10^{32} *erg.*
- Several issues/caveats:
  - *NLFFF calculations do not reach a consensus for this case*. A greater degree of robustness is desired before stronger conclusions can be drawn.
  - *Best-fit model did not provide a perfect match to EUV and X-ray loops. The lack of a proper quantitative best-fit metric makes it hard to determine best-fit model unambiguously.*
  - *Lower boundary did not fully contain both flare ribbons*, which may be associated with additional current systems used to power the eruption.

Solar study II

- We performed extrapolations based on Hinode/SOT-SP vector magnetogram scan of AR 10953 on 30 Apr. 2007.
  [DeRosa et al, submitted to ApJ on 13 Nov. 2008.]

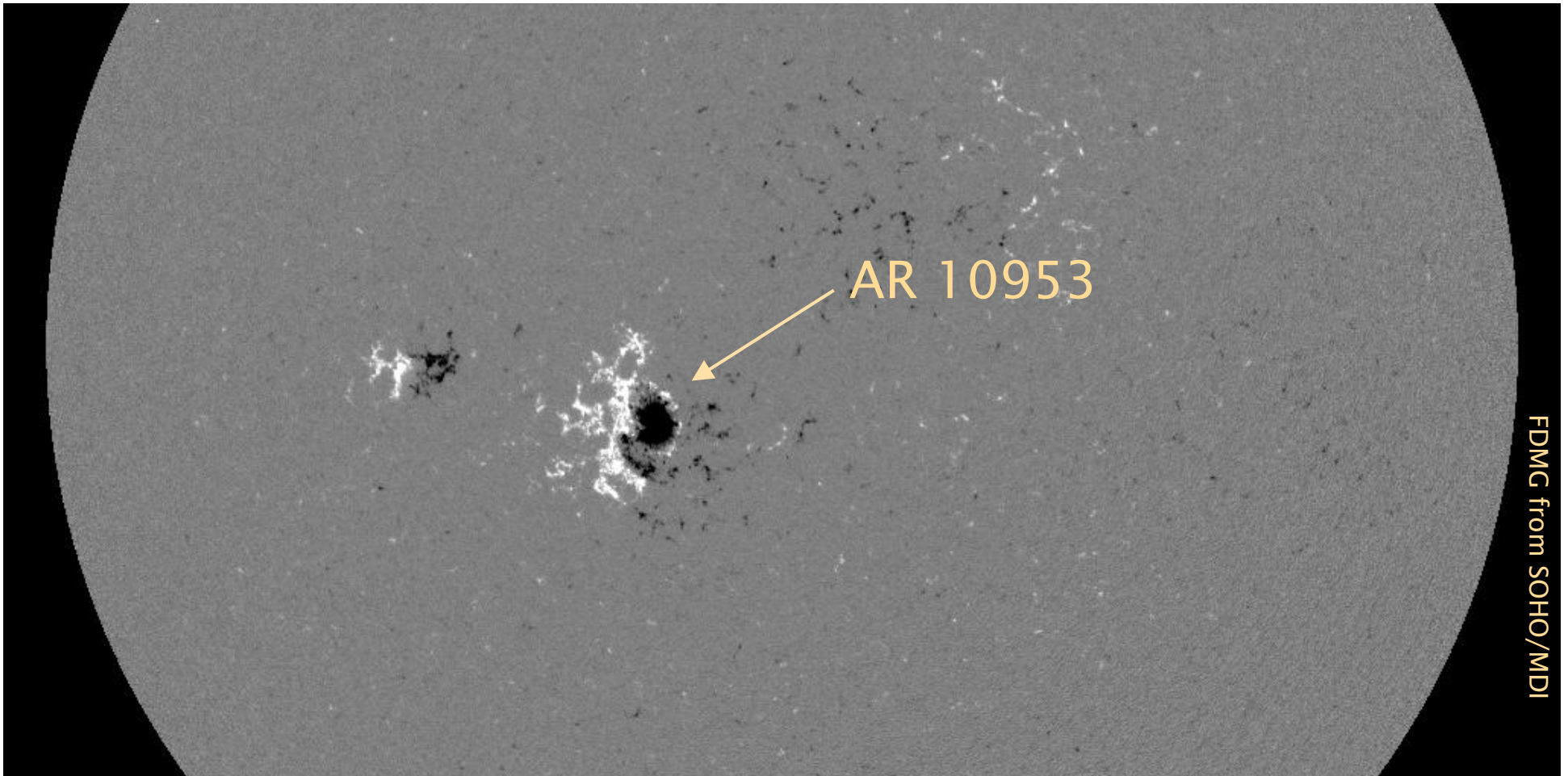

STEREOscopic imaging available

- STEREO A&B data were used for a quantitative comparison of the models with the coronal loop traces:

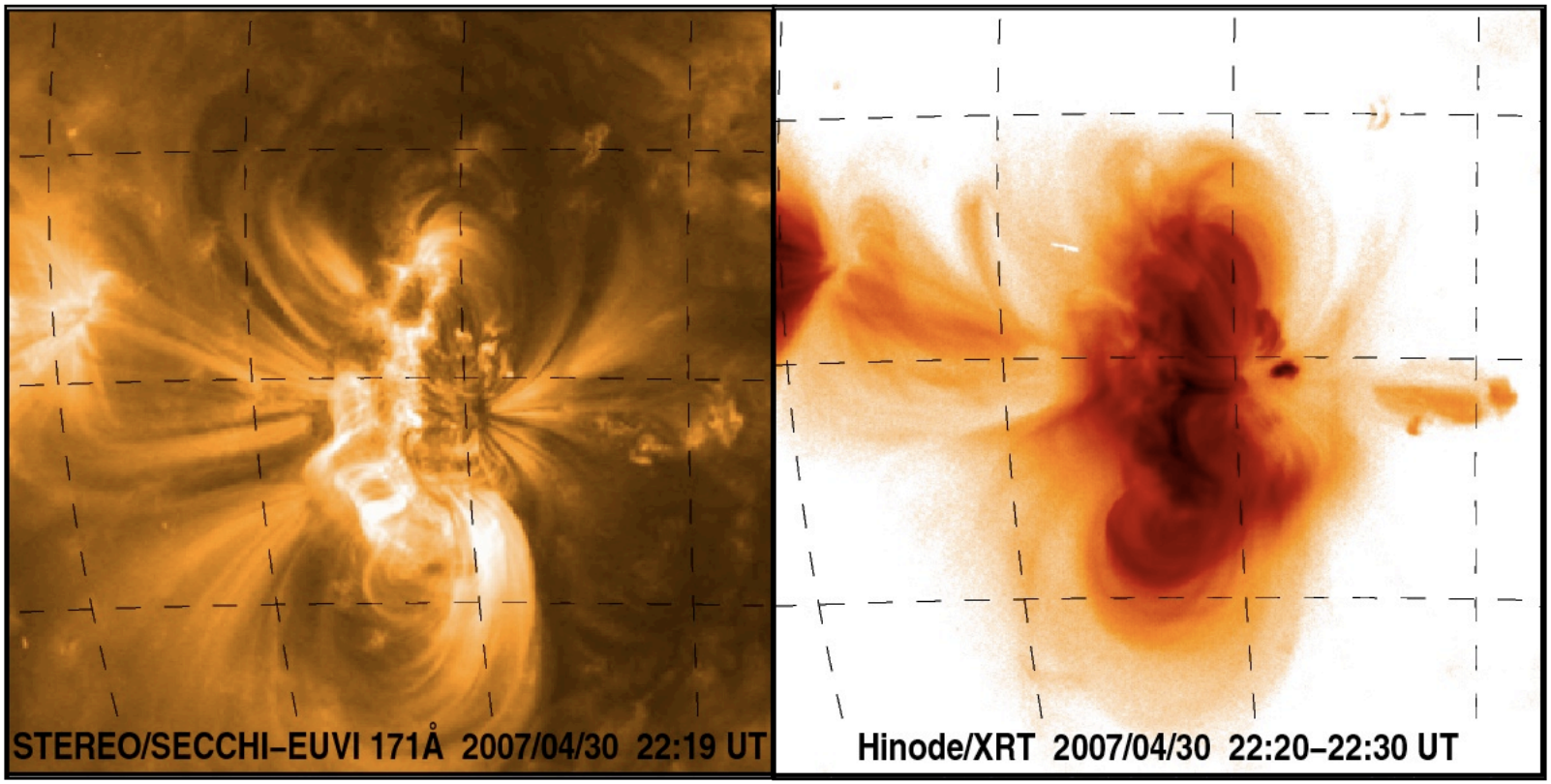

Best fit to STEREO data:

- The best fit model to the STEREO loop traces matches no better than the potential field, and does not contain a flux-rope or arcade-like filament configuration.

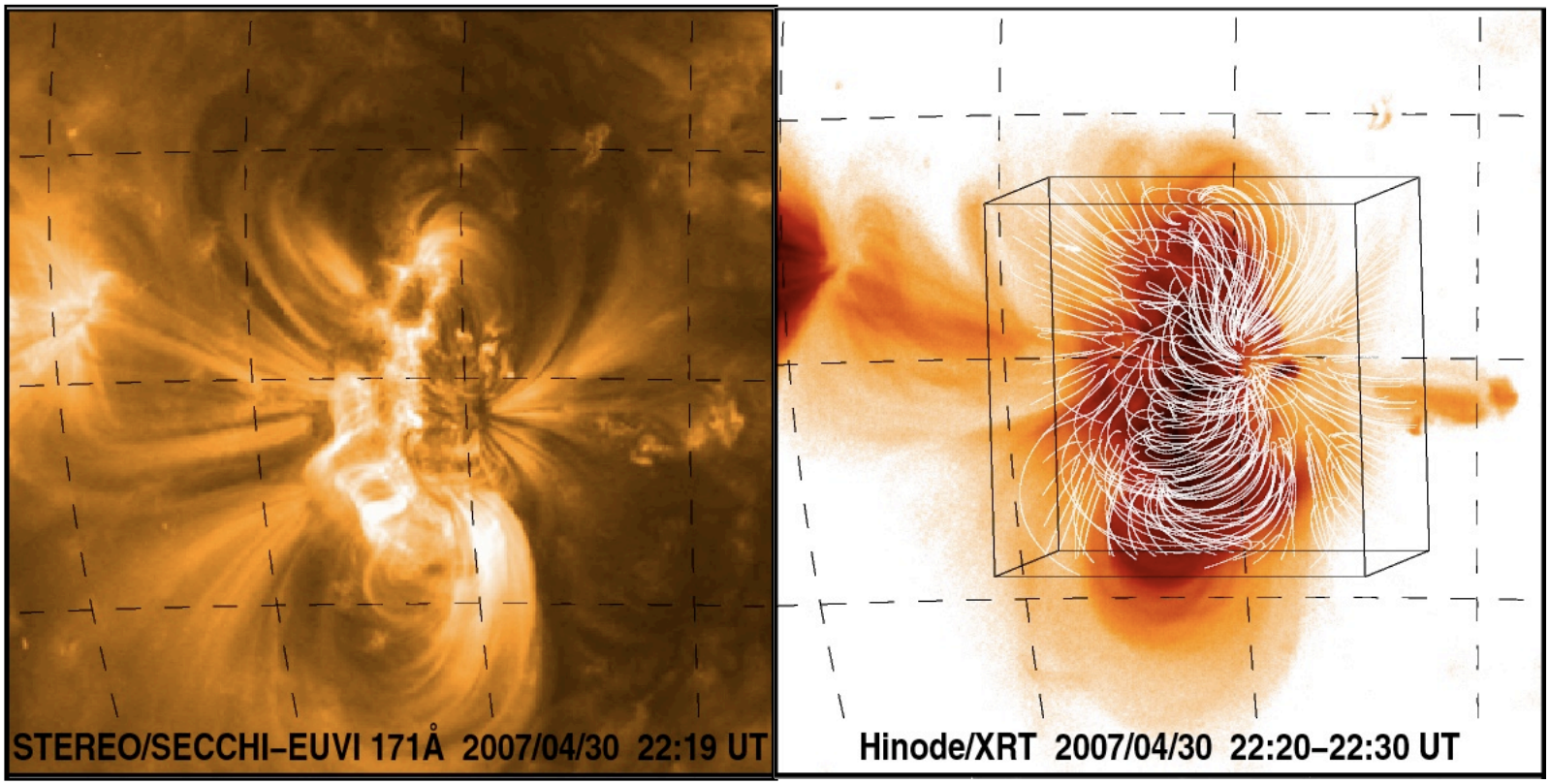

Table of metrics for AR 10953

TABLE 1

FIELD EXTRAPOLATION METRICS[a] FOR AR 10953

Model[b]	$E/E_{\rm pot}$ [c]	$\langle \mathrm{CW}\sin\theta\rangle$ [d]	$\langle\lvert f_i\rvert\rangle$ [e] ($\times 10^8$)	$\langle\phi\rangle$ [f]
Pot	1.00	—	0.02	24°
Wh^+	1.03	0.24	7.4	24°
Tha	1.04	0.52	34.	25°
Wh^-	1.18	0.16	1.9	27°
$\mathrm{Am1}^-$	1.25	0.09	0.72	28°
$\mathrm{Am2}^-$	1.22	0.12	1.7	28°
Can^-	1.24	0.09	1.6	28°
Wie	1.08	0.46	20.	32°
McT	1.15	0.37	15.	38°
$\mathrm{Rég}^-$	1.04[g]	0.37	6.2	42°
$\mathrm{Rég}^+$	0.87[g]	0.42	6.4	44°
Val	1.12	0.19	99.	—

Comparison with STEREO

- We compared model field lines to three-dimensional loop trajectories determined using stereoscopic analysis of STEREO/SECCHI-EUVI observations.
- Alignment: $\phi < 5°$ (yellow), $\phi > 45°$ (red)

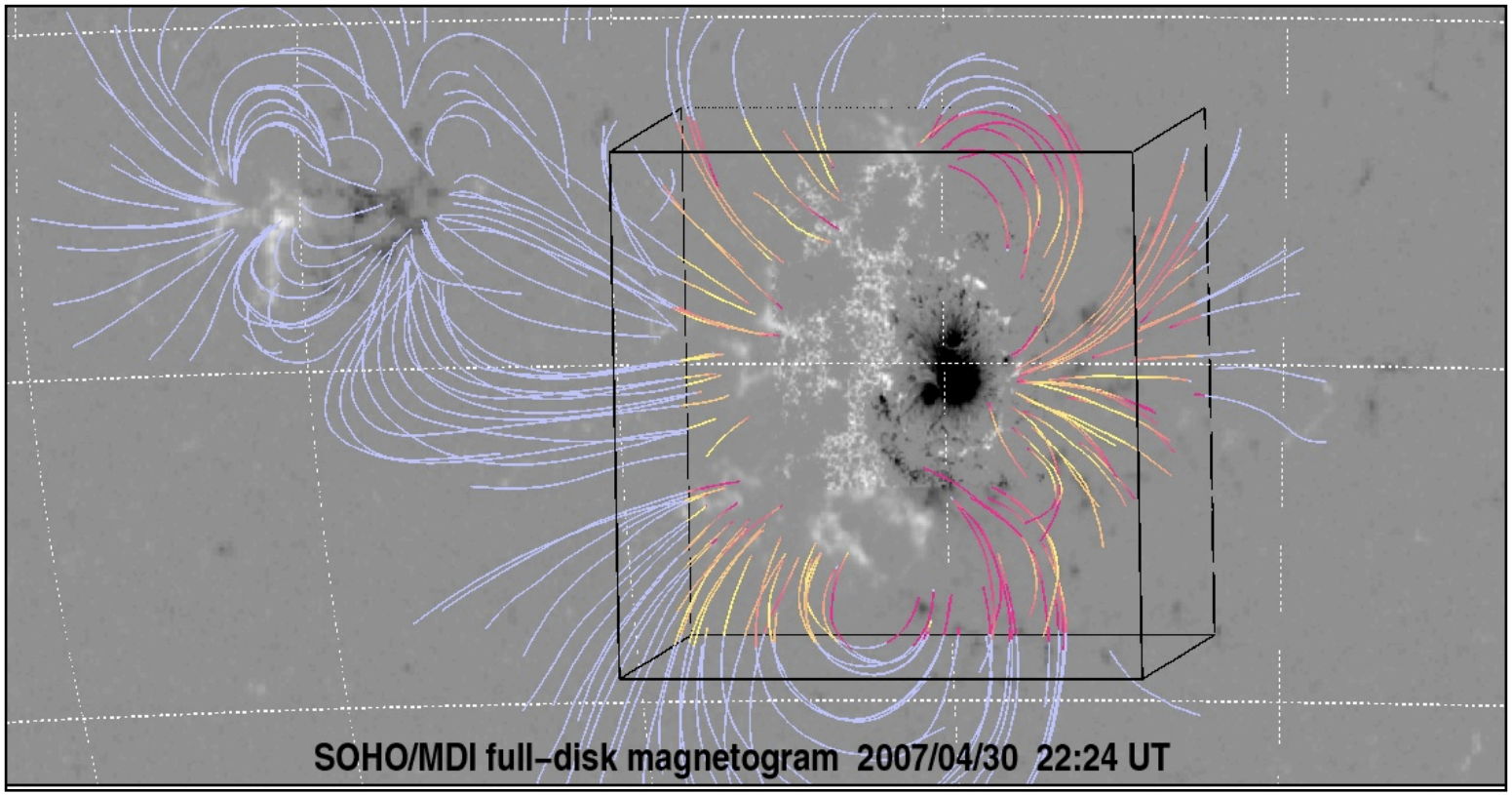

Appearances

- XRT (soft X-ray) images do not have enough structure to differentiate quantitatively, while EUV images show few (or no) loops in AR cores.
- Appearance of Amari&Canou's FEMQ (and XTRAPOL) solutions have a flux rope-like configuration near the site of a small filament (seen in Hα) which lies largely outside the vector-field map.

Potential field overlay

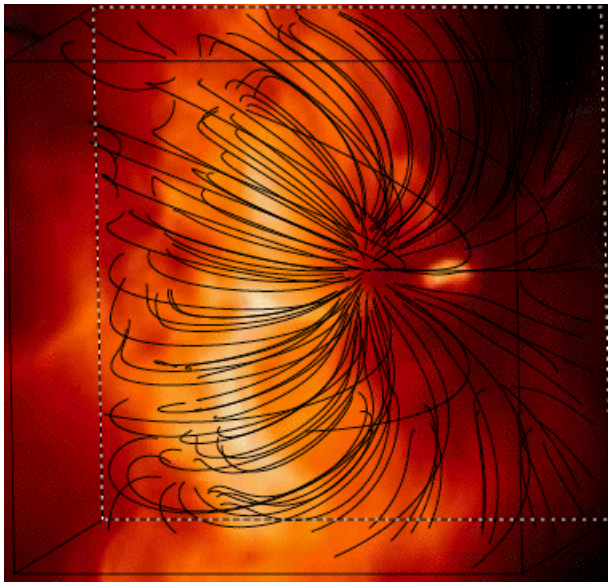

Wheatland-negative solution

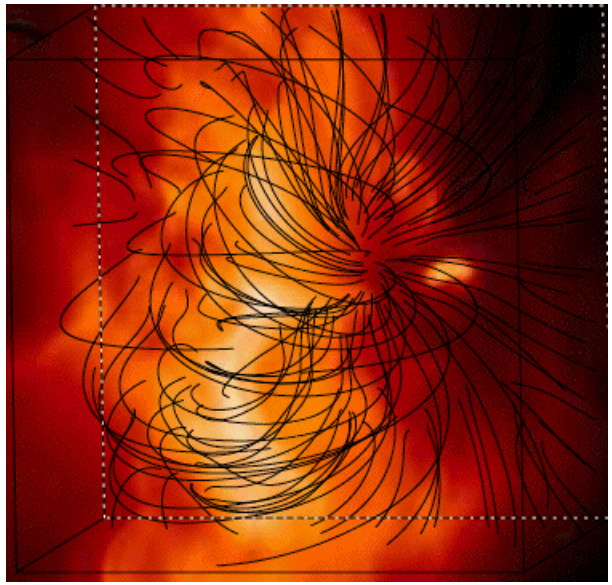

Amari-FEMQ solution

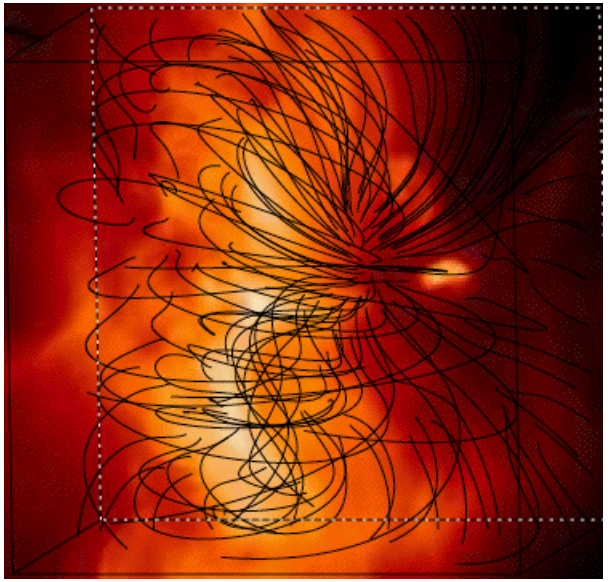

Line-of-sight integrated currents

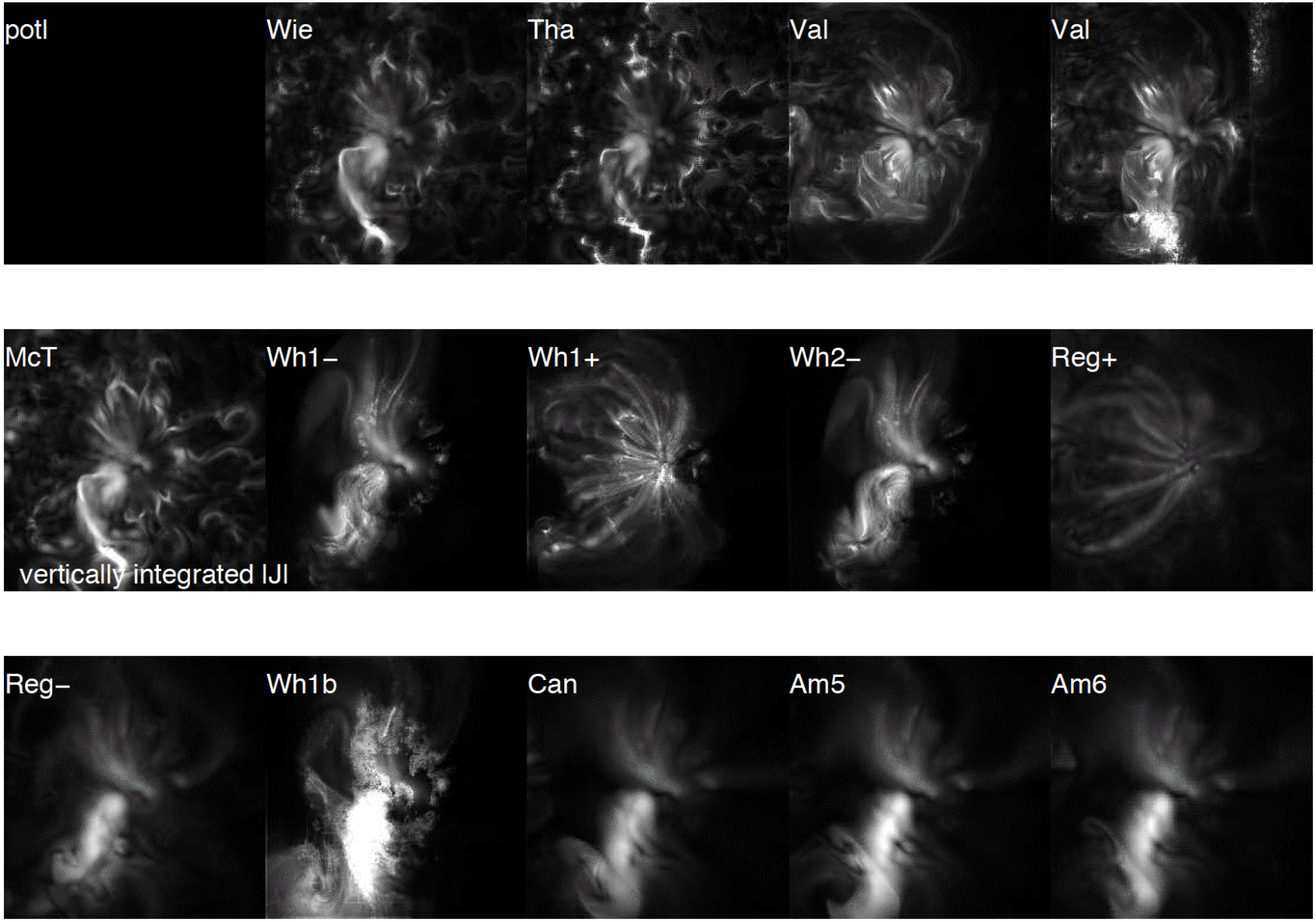

"Censoring" the observations

- *Observed vector magnetic field is inconsistent with basic requirements of force-freeness and alpha-flux balance.* Preprocessing removes net force and torque, but does not remove these two inconsistencies.
- *The algorithms deal with this in different ways*: some select/censor the data, others introduce sources of flux and current, some modify/ignore the top and side boundaries.

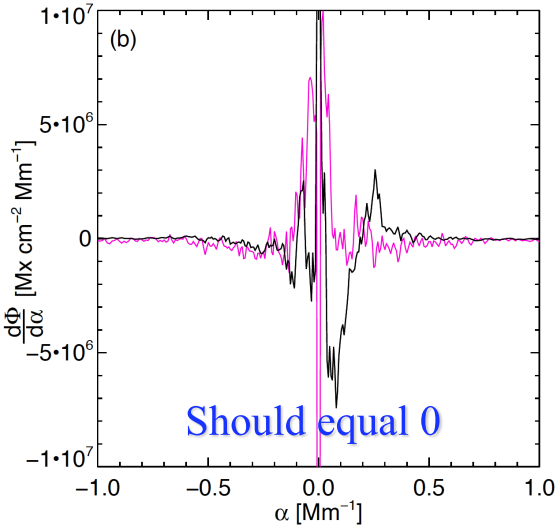

Net flux between α and α+dα should be zero. This is not true for observed (purple) or pre-processed (black) vector field.

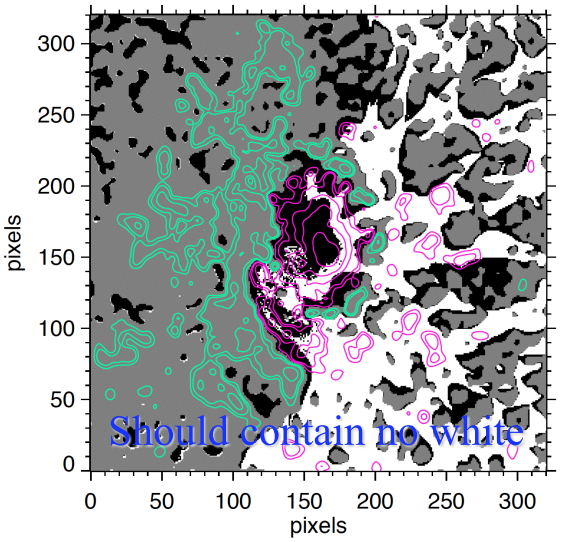

"Censoring" is one way to deal with inconsistency: Wh only uses α in the black areas, setting α =0 in white regions, disregarding the oppositepolarity (gray).

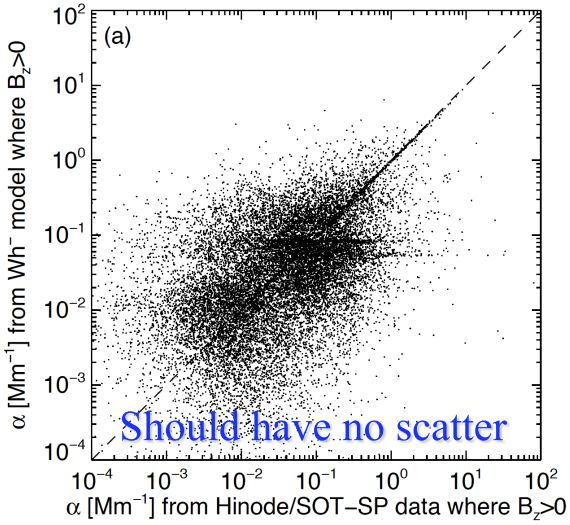

The ideal solution would connect points with matching α values. A poor model, or a highly-structured α map, shows scatter.

Forces near the lower boundary:

- Forcing the field can significantly alter the solution of the field. See linear magnetostatic field model by Low (1992)

Potential field *Forced: a = 1.0* *2.0* *3.0* *4.0; at fixed α*

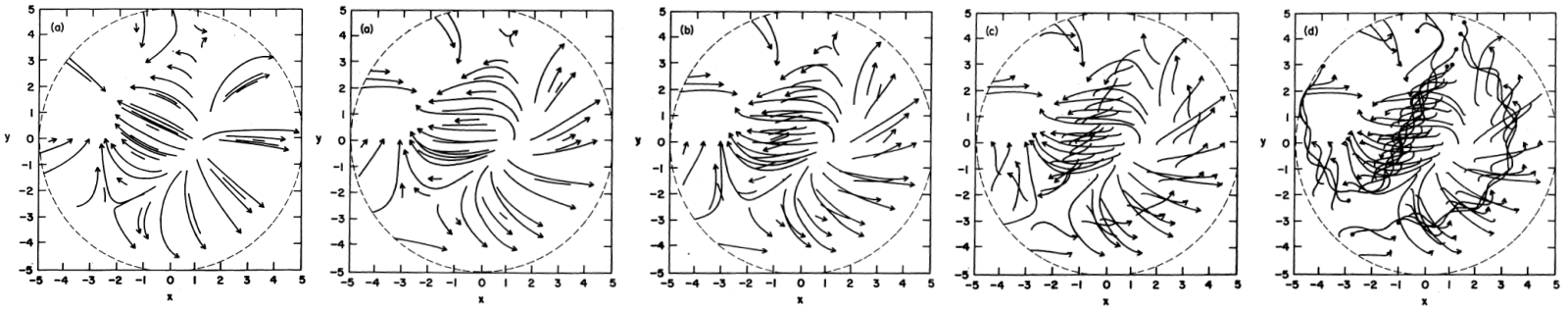

FIG. 6.—Lines of force seen in vertical projection on the plane $z = 0$ of the non–force-free magnetic fields with $a = 1.0, 2.0, 3.0, 4.0$ in panels *a*, *b*, *c*, and *d*, respectively, and $\alpha_0 = 0.4$ in all four cases.

- Some NLFFF models work quite well for a force-free boundary field (see Metcalf et al., Solar Physics 247, 269 [2008])

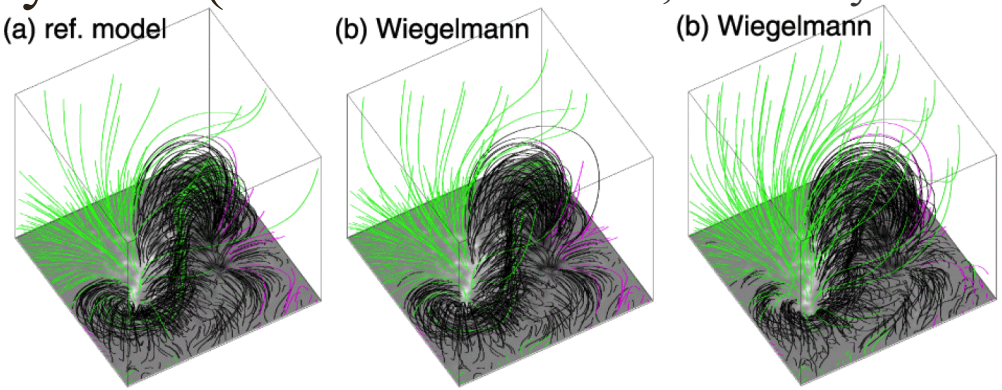

Reference model From “chromosphere” From “photosphere”

Low (1992)

Critical problem areas in NLFFF modeling

- No quantitative metric for goodness-of-fit available for the core domain of active regions.
- Observed magnetic field is inconsistent with the NLFFF model:

1. Photosphere has Lorentz and buoyancy forces.
   - Observations are inconsistent with model assumption.
   - All codes have trouble converging/optimizing when applied to forced boundary data.
   - Some codes performed well when applied to force-free cases with known solar-like solutions.
2. Preprocessing is an attempt to mitigate this inconsistency
   - Boundary (substantially) altered to minimize net force and torque.
   - Laplacian smoothing is applied.
   - Results are better with preprocessing than without.
   - Including directional information on chromospheric fibrils does not suffice (although it did in a numerical test case).
   - The “pre-processing” is only one of many possible such manipulations - needs work.

Status of NLFFF modeling

- Active, committed globe-spanning NLFFF team.
- Increased appreciation of the magnitude of the problem.
- (Some, perhaps all) *NLFFF algorithms work in principle*, but - not surprisingly - *they are very sensitive to boundary (and initial) conditions*.
- Several models *improved incorporation of boundary conditions.*
- During the NLFFF-team project, *resolutions advanced from 64^3 to over 320^3*.
- *Some spherical-coordinate versions are being tested*.
- Provided guidance for observations:
  - Large fov at high resolution [see next page];
  - X-ray and EUV observations for model validation.

Improving the modeling

a) We need a physically realistic description (and measurements) of the photosphere-corona interface, ideally with guidance from chromospheric (vector-)magnetic observations. Hα fibril directions only appears to be insufficient, although we may still find them helpful with chromospheric l.o.s. field.

b) Vector-magnetic maps need to *include all substantial connections (for flux and currents) of an active region to its surroundings* at least every few hours, and for flux emergence at least every ~0.5h. A large fov is likely as critical as high resolution: *f.o.v. >10 × AR area, resolution <1".*

c) Codes need to *accommodate uncertainties in the boundary field*.

d) e) f) …

Improving the modeling

a) b) c) …

b) We need *more inter-comparisons of NLFFF algorithms* to better understand their responses to inconsistent, incomplete, imperfect boundary and initial conditions; and to understand if model-field differences point to algorithm problems, to intrinsic limitations to extrapolations, or forces, or non-uniqueness.

c) Use *high-fidelity radiative-MHD simulations* of active regions and associated polarization signals to perform NLFFF experiments to understand impacts of various effects.

d) We need a *quantitative metric for the goodness-of-fit* of NLFFF models to the observed corona to enable iterative improvement of NLFFF models. Stereoscopic imaging at 3-5MK emissions would help.

Recommendations for Solar-C(B)

- In my opinion:
  - If the science focus is primarily coronal (e.g., field instability, coronal heating, coronal seismology, …), then Solar-C instrumentation should enable:
    - Large area spectro-polarimetric observations, large-area high-resolution (photospheric and chromospheric), narrow band coronal imaging, plus question-specific instrumentation.
  - If the science focus is primarily surface-to-corona coupling, then Solar-C instrumentation should focus on
    - High-resolution (space, time, and "depth") spectro-polarimetric observations, and rapid (E)UV/optical spectrography, plus low coronal imaging and perhaps spectrography.
  - If both, Solar-C instrumentation should have both sets of capabilities rather than a compromising compromise.